Available online at www.sciencedirect.com

ScienceDirect

journal homepage: www.elsevier.com/locate/he

Comparative study on the effect of CO_2 and H_2O dilution on laminar burning characteristics of CO/H_2/air mixtures

Yongliang Xie, Jinhua Wang, Nan Xu, Senbin Yu, Zuohua Huang**

State Key Laboratory of Multiphase Flow in Power Engineering, Xi'an Jiaotong University, Xi'an 710049, PR China

ARTICLE INFO

Article history:
Received 28 October 2013
Received in revised form
28 November 2013
Accepted 5 December 2013
Available online 4 January 2014

Keywords:
Syngas
CO_2 dilution
H_2O dilution
Chemical kinetics
Flame instability

ABSTRACT

A study on the effect of CO_2 and H_2O dilution on the laminar burning characteristics of CO/H_2/air mixtures was conducted at elevated pressures using spherically expanding flames and CHEMKIN package. Experimental conditions for the CO_2 and H_2O diluted CO/H_2/air/mixtures of hydrogen fraction in syngas from 0.2 to 0.8 are the pressures from 0.1 to 0.3 MPa, initial temperature of 373 K, with CO_2 or H_2O dilution ratios from 0 to 0.15. Laminar burning velocities of the CO_2 and H_2O diluted CO/H_2/air/mixtures were measured and calculated using the mechanism of Davis et al. and the mechanism of Li et al. Results show that the discrepancy exists between the measured values and the simulated ones using both Davis and Li mechanisms. The discrepancy shows different trends under CO_2 and H_2O dilution. Chemical kinetics analysis indicates that the elementary reaction corresponding to peak ROP of OH consumption for mixtures with CO/H_2 ratio of 20/80 changes from reaction R3 ($OH + H_2 = H + H_2O$) to R16 ($HO_2+H = OH + OH$) when CO_2 and H_2O are added. Sensitivity analysis was conducted to find out the dominant reaction when CO_2 and H_2O are added. Laminar burning velocities and kinetics analysis indicate that CO_2 has a stronger chemical effect than H_2O. The intrinsic flame instability is promoted at atmospheric pressure and is suppressed at elevated pressure for the CO_2 and H_2O diluted mixtures. This phenomenon was interpreted with the parameters of the effective Lewis number, thermal expansion ratio, flame thickness and linear theory.

1. Introduction

With the increasing concern on environmental protection, more stringent legislation has been imposed on vehicle exhaust gas emissions and the research on clean combustion have drawn much attention in recent years. IGCC (Integrated Gasification Combined Cycles) is one of the most promising technologies for future efficient and clean energy system. For IGCC power plant, coal or other fuels are gasified and the product is called syngas, with main compositions of CO and H_2 [1]. Syngas can be burned in gas turbine for power generation and it can be also used for other combustion devices such as internal combustion engines and/or cook appliance. Though IGCC can reduce most pollutant emissions greatly, the NOx emission is still a challenge due to high-temperature reaction of N_2. EGR (Exhaust Gas Recirculation) has been widely used in internal combustion engines and gas turbine to reduce the

* *Corresponding authors*. Fax: +86 29 82668789.
E-mail addresses: jinhuawang@mail.xjtu.edu.cn (J. Wang), zhhuang@mail.xjtu.edu.cn (Z. Huang).
0360-3199/$ – see front matter
http://dx.doi.org/10.1016/j.ijhydene.2013.12.037

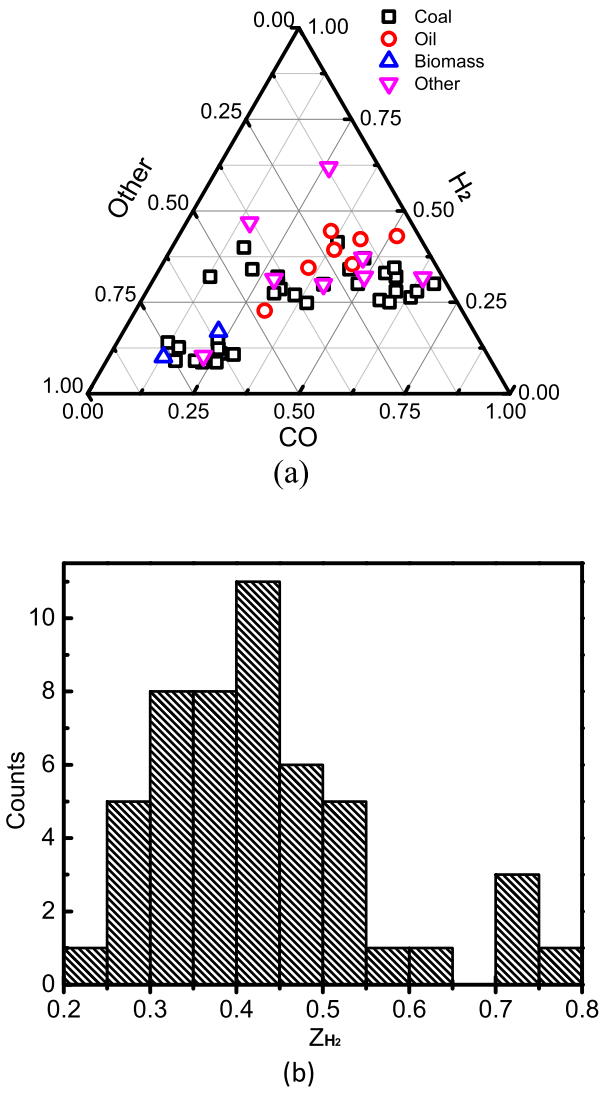

Fig. 1 – The summary of syngas composition for various fuel resources and gasification systems [10,11] ($ZH_2 = XH_2/(XH_2 + XCO)$, X represents mole fraction of specific species in the mixtures).

NOx emission due to decrease of flame temperature [2–5]. However, the flame characteristics for individual effect of EGR gas component especially CO_2 and H_2O with different thermal diffusivities and participation in chemical reaction are not well understood. For turbulent flame, the effects of CO_2 and H_2O dilution on flame characteristics were studied extensively [6–8]. A comparative study on flame front structure of turbulent premixed flames diluted with CO_2 and H_2O has been conducted by the authors [8]. It showed that flame front structure of the turbulent premixed flames varied greatly with CO_2 dilution, but remained almost unchanged with H_2O dilution. This indicated that the effects of CO_2 and H_2O dilution on flam-turbulence interaction are significantly different. However, the different effects of CO_2 and H_2O on turbulent combustion are still far from well understood. Turbulent premixed flame combines the interaction between turbulent flow and chemical reaction of laminar flame. Fundamental parameters of laminar flame, such as laminar burning velocity and flame instability are essential to the understanding of turbulent combustion. Thus, the systematical study on the diluted CO_2 and H_2O laminar flame characteristics is indispensable for better understanding of the different effects of CO_2 and H_2O dilution on turbulent flame.

Meanwhile, one of the main challenges for IGCC is the syngas composition variability. The specific composition of syngas depends on the fuel resources and processing condition and has a large range of variability. Fig. 1 shows the summary of the syngas composition obtained from the different fuel resources and gasification systems [9,10]. CO/H_2 ratios of syngas can vary from 20/80 to 80/20. Hydrogen enrichment and large variability of syngas composition complicate the design of combustion chamber which is much different from that of hydrocarbon fuels. Furthermore, combustion processes will be even complicated for syngas with EGR dilution.

Laminar burning characteristics of the syngas diluted with CO_2 and H_2O were separately studied previously. Using Bunsen burner, Natarajan et al. [11] experimentally measured the laminar burning velocities of lean syngas with different CO/H_2 ratios, at temperature of 700 K and pressure of 0.5 MPa. Prathap et al. [12] measured the laminar burning velocities and studied the intrinsic flame instability at a specified CO/H_2 ratio (50/50), temperature of 302 K and pressure of 1.0 atm using a spherically expanding flame. Ratna et al. [13] reported laminar burning velocities and flame instability of the syngas diluted with CO_2 at 303 K and 1.0 atm, using the heat flux method. Laminar burning characteristics of the H_2O diluted syngas were also been examined. Krejci et al. [14] measured the laminar burning velocities of moist syngas at various temperatures (323–423 K) and pressures (0.1–1.0 MPa) using the spherically expanding flame. Das et al. [15] experimentally measured the laminar burning velocities of moist syngas at normal pressure and temperature using the counterflow twin-flame, but only lean mixture was studied. Thus, it can be seen that the study on the effect of H_2O dilution on flame instability is limited and the comparative study on the effects of CO_2 and H_2O dilution did not reported yet.

The objective of this study is to further clarify the difference of CO_2 and H_2O dilution on syngas combustion. Laminar burning velocities of CO_2 and H_2O diluted syngas were measured and simulated. Comparative analysis on chemical kinetics was made. In addition, intrinsic flame instability with CO_2 and H_2O dilution was analyzed combined with flame propagating images and linear flame instability theory.

2. Experimental and simulation method

Detailed description of the experimental apparatus has been given elsewhere [16,17]. The system mainly composes of a constant volume combustion chamber, ignition electrodes, heating system, high-speed schlieren photography and data acquisition system. The combustion occurs in the cylindrical combustion chamber which equips two quartz windows with diameters of 80 mm. Two windows are separately located on the front and reverse side of the cylinder for optical access. In experiment, the combustible mixture in the combustion

chamber was heated by the heating tape wrapped around the chamber and the temperature was controlled by a thermocouple with an uncertainty of ±3 K. Then the combustible mixture was ignited by the centrally located electrodes and flame propagation process was imaged with schlieren technique and high speed camera (Phantom V611).

For an outwardly spherical propagating flame, the stretched flame velocity, S_n, can be directly extracted through the raw flame obtained from experiments [18,19],

$$S_n = \frac{dr_u}{dt} \tag{1}$$

where r_u represents the radius of spherical flame.

Overall stretch rate of spherical flame, α can be calculated through

$$\alpha = \frac{d(\ln A)}{dt} = \frac{1}{A}\cdot\frac{dA}{dt} = \frac{2}{r_u}\cdot\frac{dr_u}{dt} = \frac{2}{r_u}\cdot S_n \tag{2}$$

For moderate stretch rates, there exists a linear relationship between overall stretch rate, α, and unstretched flame propagation speed, S_b [18,20],

$$S_b - S_n = L_b\cdot\alpha \tag{3}$$

where L_b is Markstein length of burned gas, and S_b can be obtained through linear regression. Laminar burning velocity, S_L, can be evaluated through the continuity equation across the flame front,

$$\rho_u S_L = \rho_b S_b \tag{4}$$

In this experiment, flame images with the radius between 5 mm and 25 mm are chosen to extract the laminar burning velocities by comprehensive consideration of effects of ignition energy and pressure change in the combustion chamber. Air was replaced by the mixture of 79%N_2 and 21%O_2 volumetrically. The fraction of CO_2 or H_2O in the diluted syngas mixtures is defined as $ZH_2O(CO_2) = XH_2O(CO_2)/XH_2O(CO_2) + XN_2 + XO_2$. Here X refers to mole fraction of the specific species in the mixtures.

One dimensional freely propagating laminar unstretched flame is simulated using the Sandia code PREMIX [21] coupled with CHEMKIN-II program [22]. Two available syngas mechanisms were chosen for the comparative study. They are the optimized syngas kinetic mechanisms of Davis et al. [23] and Li et al. [24]. The mechanism of Davis et al. includes 6 species and 38 reactions and the mechanism of Li et al. has 21 species and 84 reactions. In this study, both GRAD and CURV parameters are set at 0.02 to ensure the result is grid independent. Multi-component transport model was chosen and soret effect was also included in the calculation [25]. In addition, highly radiative characteristic of CO_2 and H_2O which may influence the laminar burning velocity could be neglected in the current study because Chen et al. have demonstrated that the effects of radiative loss on spherical flame propagation can be neglected when the laminar burning velocity is above 15 cm/s [26].

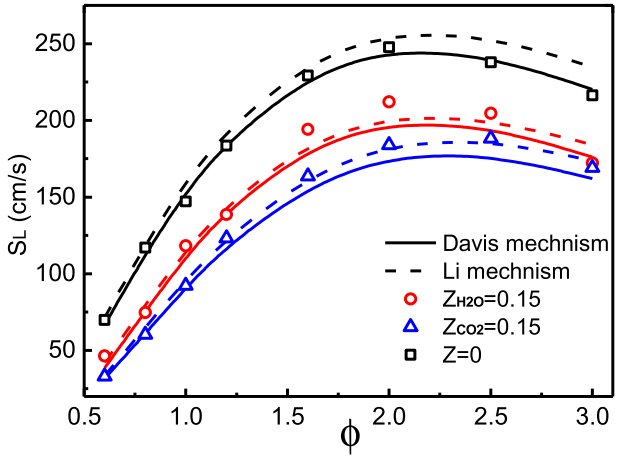

Fig. 2 – Laminar burning velocities of CO/H_2/air mixtures with CO_2 and H_2O dilution ($T = 373 \pm 3$ K, $p = 0.1$ MPa, $CO/H_2 = 50/50$).

3. Results and discussion

3.1. *Laminar burning velocities of the CO_2 and H_2O diluted CO/H_2/air mixtures*

Fig. 2 shows the laminar burning velocities of CO_2 and H_2O diluted CO/H_2/air mixtures at various equivalence ratios. Meanwhile, the simulated ones with the mechanism of Davis et al. and the mechanism of Li et al. are also presented for the comparison. It is obvious that simulation with the mechanism of Li et al. is slightly higher than that with the mechanism of Davis et al. In general, the simulated values are in reasonable agreement with the experimental ones. In the case of no dilution, simulation with the mechanism of Davis et al. shows good agreement with the experiment. Discrepancy appears with the mechanism of Li et al. which gives slightly higher values to those of measured ones at all equivalence ratios. In the case of H_2O dilution, the phenomenon is quite different. Both the mechanism of Davis et al. and the mechanism of Li et al. can well predict the laminar burning velocities of fuel-lean mixture, but under-prediction for the fuel-rich mixtures. The mechanism of Li et al. has better predictability than that of the mechanism of Davis et al. In the case of CO_2 dilution, the calculated data with the mechanism of Li et al. show good agreement with the experimental data. The mechanism of Davis et al. under-predicts the laminar burning velocities at all equivalence ratios. In addition, it is observed that addition of CO_2 and H_2O can both decrease the laminar burning velocity at all equivalence ratios and CO_2 dilution seems more effective in reducing laminar burning velocity than H_2O dilution.

Fig. 3 gives laminar burning velocities and maximum mole fraction of H + OH at various CO/H_2 and dilution ratios. Laminar burning velocity is deceased with the increase of CO/H_2 and dilution ratios and this is more obvious for CO_2 addition. Chen et al. [27] stated that the effects of dilution on laminar burning velocity were mainly from thermal and chemical aspects. Fig. 4 gives the adiabatic flame temperature of the CO_2 or H_2O diluted mixtures at different CO/H_2 ratios. With the increase of CO_2 and/or H_2O dilution ratio, adiabatic flame temperature presents an approximately linear decreasing trend. Similar to the laminar burning velocity, adiabatic flame temperature gives a larger decreasing in the

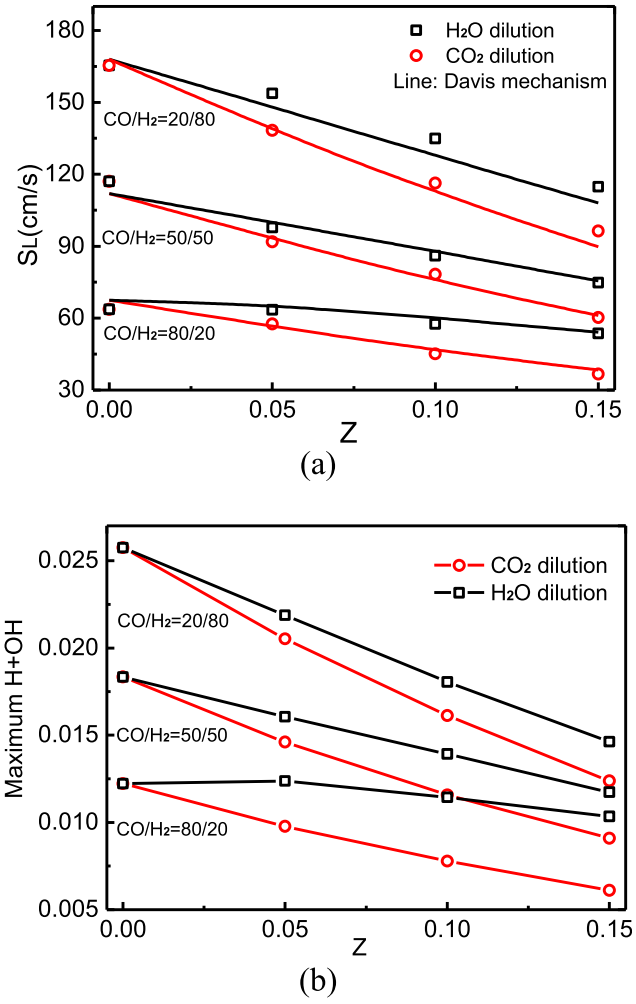

Fig. 3 – Laminar burning velocities and maximum mole fraction of H + OH of CO/H_2/air mixtures at various CO/H_2 and dilution ratios (T = 373 ± 3 K, p = 0.1 MPa ϕ = 0.8): (a) laminar burning velocities; (b) maximum mole fractions of H + OH.

case of CO_2 addition compared with H_2O dilution. However, adiabatic flame temperature increases with the increase of CO/H_2 ratios and this is different to that of laminar burning velocity.

Key free radicals (H, OH and O) are often used to analyze the chemical effect of dilution [28]. Fig. 3 shows that variation of maximum H + OH concentration has the similar trend with that of laminar burning velocities of CO_2 or H_2O dilution. Maximum H + OH concentration is decreased when CO_2 and/or H_2O are added. This indicates that the free radicals (especially H and OH) are extremely important to laminar burning velocity since the concentration of those radicals plays an important role in the elementary reactions. In fact, previous researches [29,30] also reported the strong correlation of laminar burning velocity with maximum concentration of H + OH radicals in the reaction zone. Thus, concentrations of free radicals can be used to study the chemical effect of the CO_2 and/or H_2O diluted syngas/air mixtures.

Fig. 5 shows the peak ROP (Rate of Production) of H and OH radicals for the CO_2 and/or H_2O diluted mixtures at different CO/H_2 ratios. When mole fraction of H_2 in syngas is low (CO/H_2 = 80/20), the greatest contribution on H production is the elementary reaction R28: CO + OH = CO_2 + H. Reaction R1: H + O_2 = O + OH is the main consumption reaction of H radical. For OH radical, the most important elementary reactions are still R1 and R28. However, R28 becomes the greatest contribution of OH consumption and R1 is the main elementary reaction that produces the OH radical. When CO_2 and/or H_2O are added, the main contributions of H and OH radicals remain the same, but peak ROP is decreased and the effectiveness of CO_2 dilution is higher than H_2O dilution. Peak ROP of H and OH slightly shift to the downstream. When mole fraction of H_2 becomes larger from 0.2 to 0.8, the dominating elementary reaction that consumes H radical remains the same but reaction R3: OH + H_2 = H + H_2O becomes the most important elementary reaction for the production of H. When CO_2 and/or H_2O are added, the dominating reactions remain unchanged with decreased peak ROP and shifting slightly to the downstream. R1 remains the most important reaction for production of OH radical in syngas/air mixtures with and without CO_2 or H_2O dilution. For the consumption of OH, however, R3, substituting R28, becomes the dominating reaction for syngas/air mixtures without dilution. Main elementary reaction for consumption of OH radical is changed from R3 to R16 when CO_2 and/or H_2O are added.

To compare the different kinetic effects of CO_2 and H_2O, the normalized sensitivity coefficient of the CO_2 or H_2O diluted CO/H_2/air mixtures is given in Fig. 6. Reaction R28 gives the largest positive sensitivity for the mixture with CO/H_2 ratio of 80/20. The third body reaction R12: H + O_2 (+M) = HO_2 (+M) gives the largest negative sensitivity coefficient. Dilution of CO_2 and H_2O has an increasing effect on the sensitivity coefficient of R12 in which the effect of CO_2 is higher than that of H_2O. When mole fraction of H_2 in syngas changes from 0.2 to 0.8, the most important positive elementary reaction is changed from R28 to R3: OH + H_2 = H + H_2O. This is consistent with the observation in Fig. 5. R12 still remains an important elementary reaction which has the negative effect on laminar burning velocity. However, the reaction R9: H + OH + M = H_2O + M, replacing reaction R12, becomes the

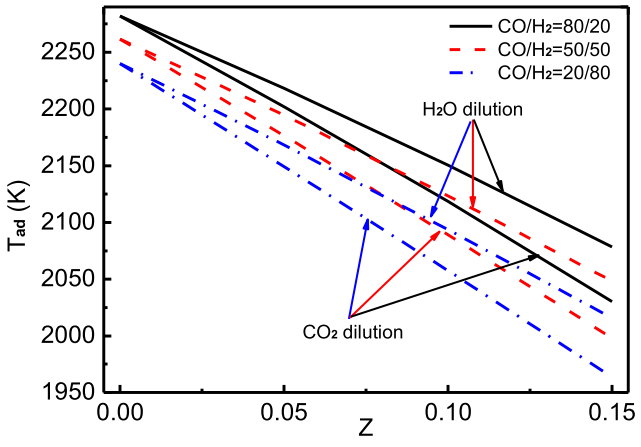

Fig. 4 – Adiabatic flame temperature of CO/H_2/air mixtures with CO_2 and H_2O dilution at various CO/H_2 ratios (T = 373 ± 3 K, p = 0.1 MPa, ϕ = 0.8).

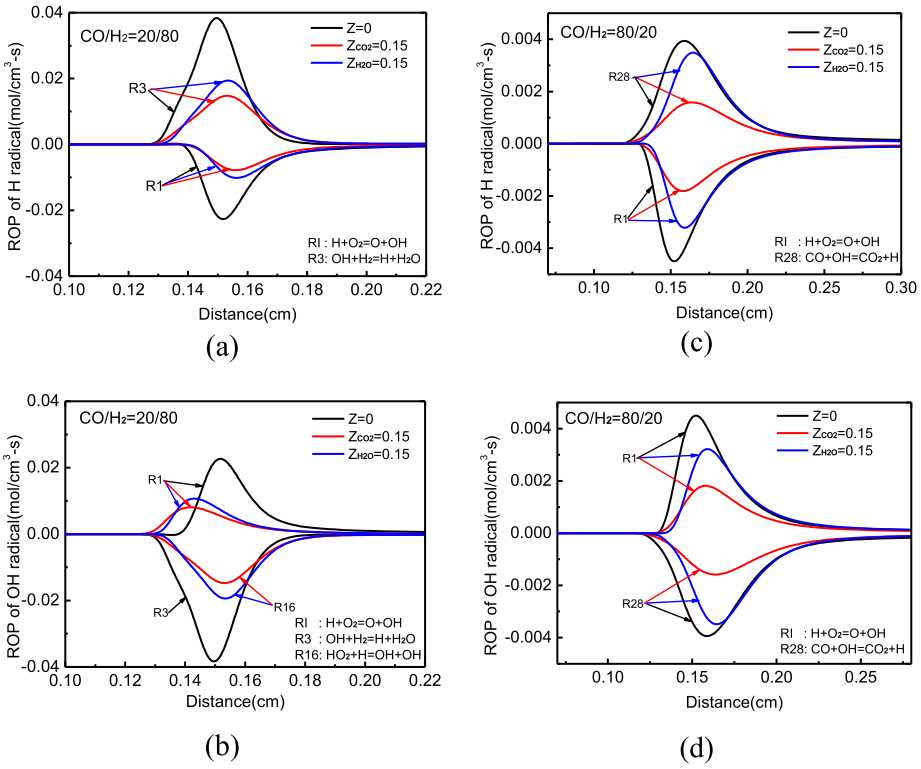

Fig. 5 – ROP of H and OH radicals for CO/H_2/air mixtures with CO_2 and H_2O dilution at various CO/H_2 ratios (T = 373 ± 3 K, p = 0.1 MPa, ϕ = 0.8): (a) CO/H_2 = 20/80; (b) CO/H_2 = 20/80; (c) CO/H_2 = 80/20; (d) CO/H_2 = 80/20.

dominating negative sensitive elementary reaction. Laminar burning velocity and chemical kinetics analysis reveal stronger effect of CO_2 than H_2O on laminar premixed flame and this links to the stronger CO_2 dilution influence on flame front structure of turbulent premixed flames than that of H_2O dilution previous study [8].

3.2. *Flame instability characteristics for CO_2 and H_2O diluted CO/H_2/air mixtures*

3.2.1. *Flame cellular instability analysis with flame images*

There are three flame intrinsic instabilities, the buoyancy-driven instability, the hydrodynamic instability and the diffusive-thermal instability [31]. Buoyancy-driven instability can be neglected in this study since it only appears at very low flame speed. Hydrodynamic instability results from thermal expansion across the flame and is characterized by flame thickness and thermal expansion ratio. Diffusive-thermal instability is caused by non-equal diffusion process between heat conduction and reactant diffusion. It can be assessed by Lewis number, which is defined as the ratio of mixture thermal diffusivity to mass diffusivity of the limiting reactant relative to abundant inert gas [32,33]. Fig. 7 gives the schlieren images of flame propagation of CO_2 and H_2O diluted CO/H_2/air mixtures at different pressures. Flame instability relevant parameters, such as effective Lewis number, flame thickness and thermal expansion ratio are also provided. It can be seen the cellular structure is developed gradually as the flame propagates outwardly and the effect of flame stretch is weakened. Cellular instability is suppressed at early stage of flame propagation because of strong effect of flame stretch. As flame radius increases, the flame stretch rate decreases and inhibiting effect on flame instability is weakened. Flame front keeps smooth and only small cracks occur at pressure of 0.1 MPa. With the increase of pressure, the irregular cellular cells occur at the flame front and the onset of wrinkling appears in earlier stage. This indicates that flame front tends to be unstable with the increase of pressure. When CO_2 and/or H_2O are added, flame front shows different trends at different pressures. When the pressure is low (0.1 MPa), addition of CO_2 and H_2O promotes the flame instability. At elevated pressure, flame instability is suppressed with CO_2 and H_2O dilution. Further analysis on flame instability will be given in the following section using relevant parameters and linear theory.

Fig. 8 presents the effective Lewis number of CO/H_2/air mixtures at different CO/H_2 ratios. Here, the effective Lewis number, Le_{eff}, is thought to be a linear relation between the single fuel Lewis number and was determined using the formulas $Le_{eff} = X_{H_2}Le_{H_2} + X_{CO}Le_{CO}$, X_i being the mole fractions of fuel species [34,35]. The effective Lewis number increases with the decrease of H_2 mole fraction in syngas and it approaches the unity at H_2 mole fraction of 80%. The reason is that H_2 is more subject to the formation of flame instability and has low Lewis number than that of CO. When CO_2 and/or H_2O are added, the effective Lewis number is slightly decreased and this phenomenon becomes obviously with CO_2 dilution. This indicates that addition of CO_2 and H_2O promote the diffusive-thermal instability of the CO/H_2/air mixtures.

Flame thickness and thermal expansion ratio are two most sensitive parameters controlling the hydrodynamic instability

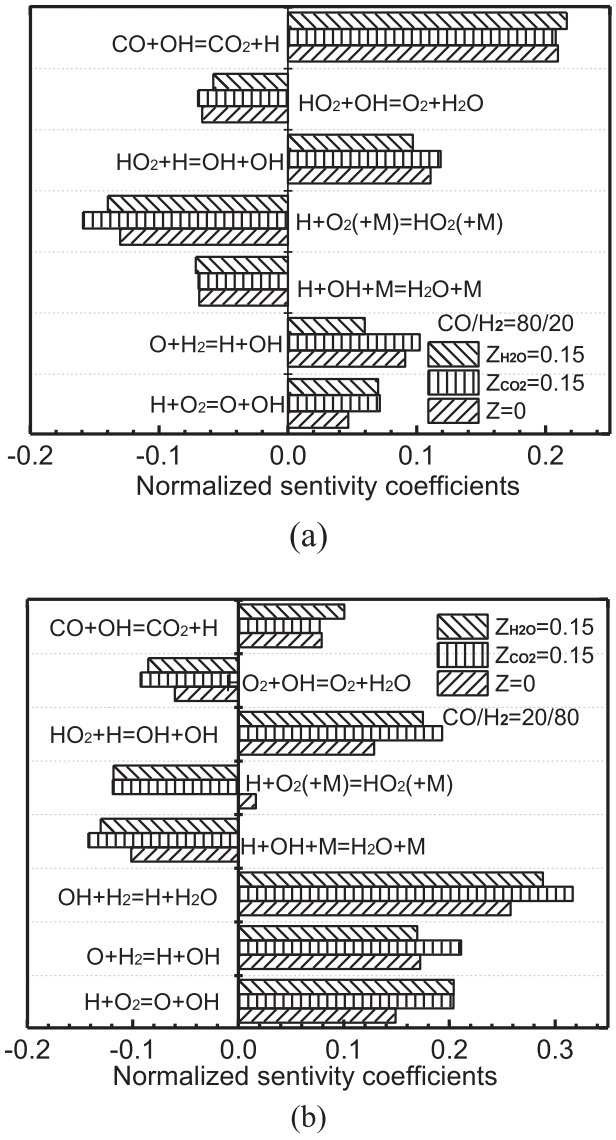

Fig. 6 – Normalized sensitivity coefficients to laminar burning velocity.

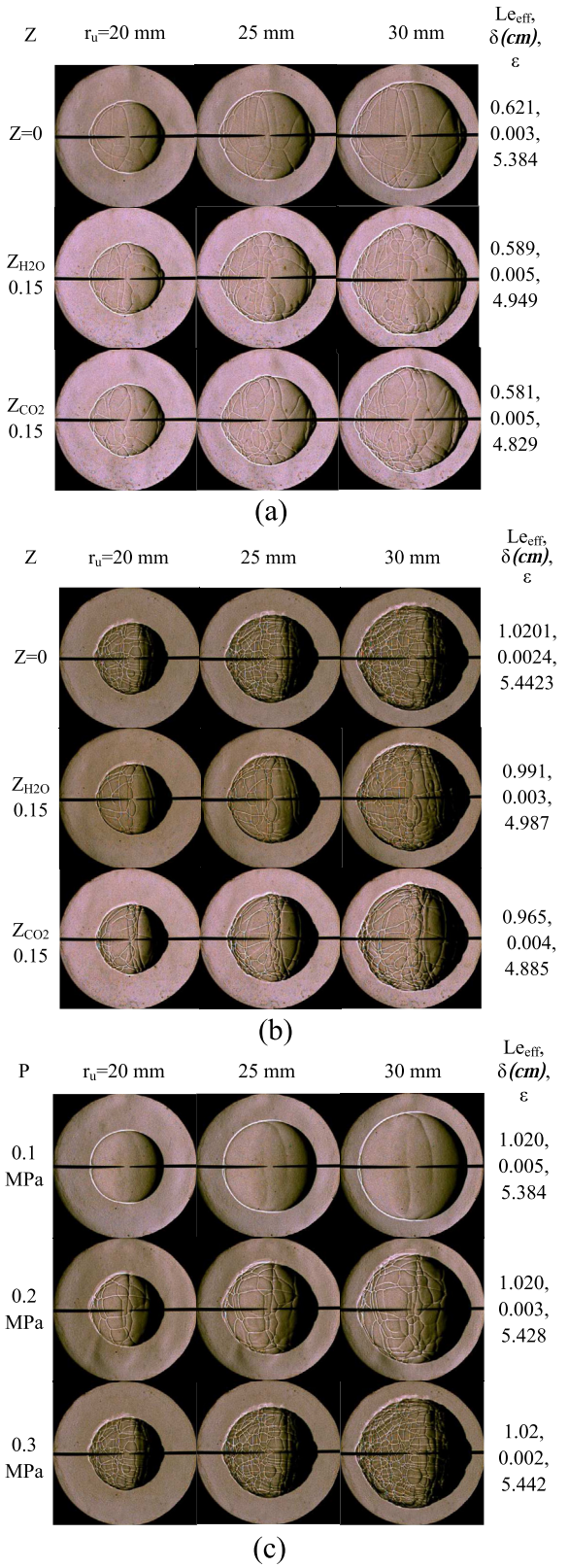

Fig. 7 – Schlieren images of CO/H_2/air mixtures with CO_2 and H_2O dilution at different pressures (T = 373 ± 3 K, ϕ = 0.8): (a) dilution effect (p = 0.1 MPa, CO/H_2 = 20/80); (b) dilution effect (p = 0.3 MPa, CO/H_2 = 80/20); (c) pressure effect (CO/H_2 = 80/20, without dilution).

[36] and are presented in Fig. 9. With the increase of H_2 mole fraction in syngas, thermal expansion ratio is increased and flame thickness is decreased. This indicates that increasing H_2 fraction in syngas can promote the hydrodynamic instability. When CO_2 and/or H_2O are added, thermal expansion ratio is decreased and flame thickness is increased. Both of them suppress the hydrodynamic instability. Compared with H_2O dilution, CO_2 dilution shows higher suppressing effect on hydrodynamic instability because of its low thermal expansion ratio and high flame thickness. Thermal expansion ratio is increased and flame thickness is decreased at elevated pressures, and this indicates the promotion of hydrodynamic instability at elevated pressure. In the early stage when flame radius is small, the hydrodynamic instability is suppressed by flame stretch and small-scale diffusive-thermal instability is a dominating factor. Thus, at pressure of 0.1 MPa, CO_2 and/or H_2O dilution promote the flame instability because of the decrease of effective Lewis number. And CO_2 dilution has

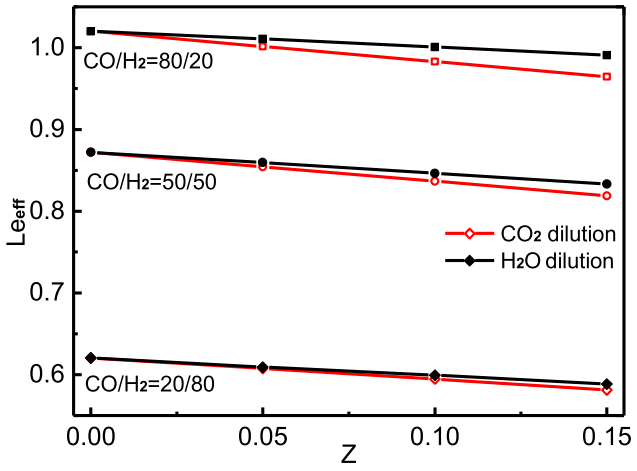

Fig. 8 – Effective Lewis number of CO/H_2/air mixtures at various CO/H_2 and dilution ratios (T = 373 ± 3 K, p = 0.1 MPa, ϕ = 0.8).

larger effect because of its lower effective Lewis number compared with H_2O dilution. As pressure is increased, the suppressing effect on hydrodynamic instability is higher than the promoting effect on diffusive-thermal stability when CO_2 or H_2O are added, thus flame front becomes smoother.

3.2.2. *Flame instability analysis with linear theory*

To better understand the cellular flame instability of the CO_2 and H_2O diluted CO/H_2/air mixtures at elevated pressure, the linear stage of flame propagation was studied. Usually, a small perturbation of a sinusoidal wave with infinitesimal amplitude is superimposed on the smooth flame front to study the flame instability [37]. Development of flame instability mainly goes through two stages, the initial linear development stage and the following nonlinear stage. During the early development of flame instability from a smooth flame front, the wavelength remains constant while the amplitude of the wave grows in exponential function of time,

$$A = A_0 e^{\sigma t} \tag{5}$$

where A_0 is amplitude of initial sinusoidal wave and σ is grow rate, which is the function of initial wave number (reciprocal of wavelength), K. Dispersion relation between σ and K is given by Yuan et al. [38] as follows,

$$\sigma = \Omega_0 S_L k - \Omega_1 \alpha k^2 - 4\alpha\delta^2 k^4 \tag{6}$$

$$\Omega_0 = \left(\sqrt{\varepsilon + \varepsilon^2 - \varepsilon^3} - \varepsilon\right) \Big/ (1+\varepsilon) \tag{7}$$

$$\Omega_1 = \frac{(1-\varepsilon)^2 - \ln\varepsilon(2\Omega_0 + 1 + \varepsilon)}{2(1-\varepsilon)[\varepsilon + (1+\varepsilon)\Omega_0]} - \frac{(1+\Omega_0)(\varepsilon+\Omega_0)\beta(1-\mathrm{Le})}{2(1-\varepsilon)[\varepsilon + (1-\varepsilon)\Omega_0]} \times \int_0^{1/\varepsilon - 1} \frac{\ln(1+\xi)}{\xi} d\xi \tag{8}$$

The first term of right side in equation (8) refers to the hydrodynamic instability, the second term refers to the diffusive-thermal instability, and the third term refers to the high-order temperature relaxation term which was added according to Sivashinsky's formulation [33]. Thus, the formulation of Yuan et al. can comprehensively reflect the combined effects of diffusive-thermal instability and hydrodynamic instability. The wave number corresponding to maximum growth rate was defined as the critical wave number, $k_{\sigma max}$. It should be noted that growth rate is smaller

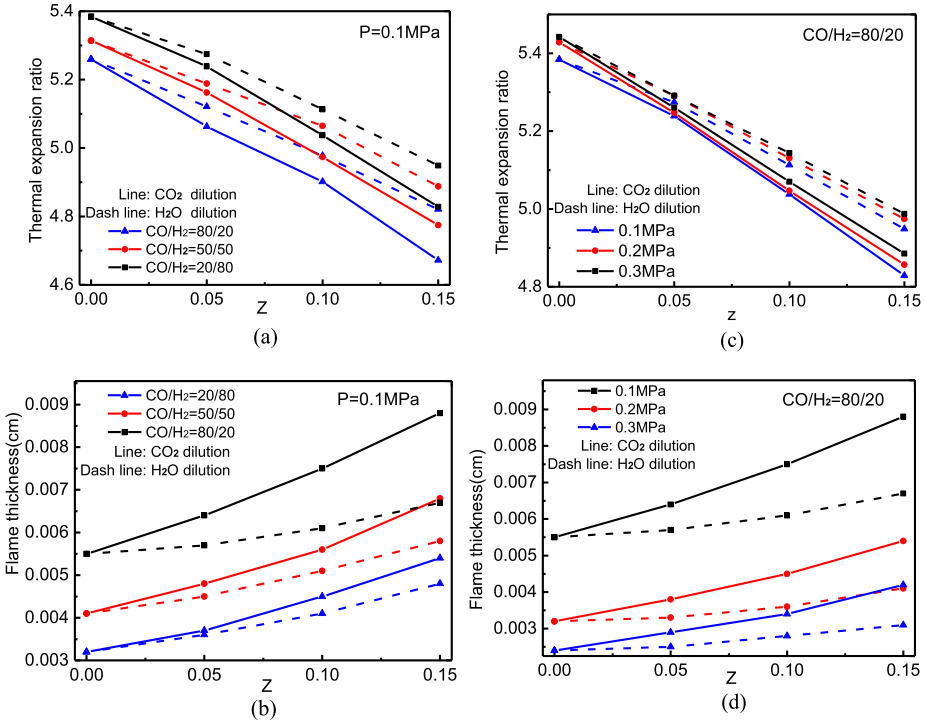

Fig. 9 – Flame thickness and thermal expansion ratio of CO/H_2/air mixtures.

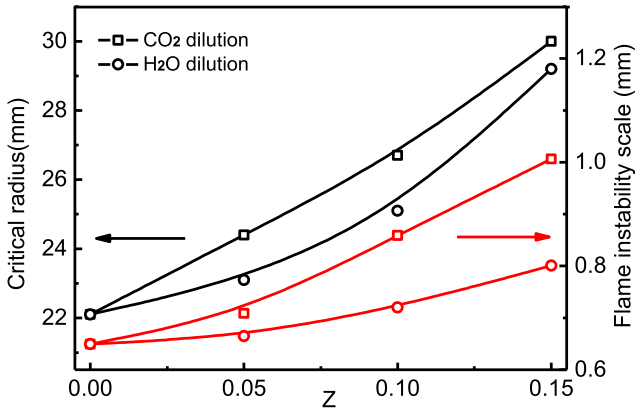

Fig. 10 – Flame intrinsic instability scale and critical radius at various dilution ratios.

than zero when wave number reaches a neutral wave number, k_n. To quantify the flame instability, the flame intrinsic instability scale, l_i, is introduced,

$$l_i = \pi / k_{\sigma_{max}} \quad (9)$$

Fig. 10 gives the flame intrinsic instability scale, l_i, and critical radius, R_{cr}, at various CO/H_2 and dilution ratios at pressure of 0.3 MPa. Here R_{cr} represents the instance where cellular structure is no longer suppressed and cells instantaneously and uniformly appear over the entire flame surface [32]. Flame intrinsic instability scale and critical radius both increases with the increase of dilution ratio. The results illustrate that addition of CO_2 and H_2O both can suppress flame instability at elevated pressure and CO_2 has a stronger inhibiting effect.

4. Conclusions

Laminar burning velocities and flame instabilities of CO_2 and H_2O diluted CO/H_2/air mixtures at different CO/H_2 and dilution ratios were investigated at elevated pressure and temperature using the outwardly spherical propagating flame. Main conclusions are summarized as follows:

1. Discrepancy exists between measured laminar burning velocities and simulated ones with the mechanism of Davis et al. and the mechanism of Li et al. For CO/H_2/air mixtures without dilution, simulated values with the mechanism of Davis et al. are in good agreement with experimental ones. In case of H_2O dilution, simulations with two mechanisms give underprediction on laminar burning velocity while the mechanism of Li et al. can give better prediction. In case of CO_2 dilution, the mechanism of Li et al. gives good prediction on the laminar burning velocity.
2. Chemical kinetic analysis shows peak ROP of H and OH and sensitivity coefficients vary significantly with CO_2 and H_2O dilution. CO_2 dilution has stronger chemical effect than H_2O dilution.
3. Intrinsic flame instability is promoted at atmospheric pressure and suppressed at elevated pressure when CO_2 and H_2O are added. Linear theory and instability parameters analysis confirm the stronger promoting or inhibiting effect of CO_2 than H_2O at atmospheric or elevated pressures.

Acknowledgments

This study is supported by National Natural Science Foundation of China (No. 51006080, 51376004) and Specialized Research Fund for the Doctoral Program of Higher Education (20130201130011). The support from the Fundamental Research Funds for the Central Universities is also appreciated. Jinhua Wang acknowledges the Japan Society for the Promotion of Science for a JSPS Postdoctoral Fellowship grant.

REFERENCES

[1] Wang J, Huang Z, Kobayashi H, Ogami Y. Laminar burning velocities and flame characteristics of CO–H_2–CO_2–O_2 mixtures. Int J of Hydrog Energy 2012;37:19158–67.
[2] Li SC, Williams FA. NOx formation in two-stage methane-air flames. Combust Flame 1999;118:399–414.
[3] Barlow RS, Karpetis AN, Frank JH, Chen JY. Scalar profiles and NO formation in laminar opposed-flow partially premixed methane/air flames. Combust Flame 2001;127:2102–18.
[4] Liu F, Guo H, Smallwood GJ, Gulder OL. The chemical effects of carbon dioxide as an additive in an ethylene diffusion flame: implications for soot and NOx formation. Combust Flame 2001;125:778–87.
[5] Kim S-G, Park J, Keel S-I. Thermal and chemical contributions of added H_2O and CO_2 to major flame structures and NO emission characteristics in H_2/N_2 laminar diffusion flame. Int J Energ Res 2002;26:1073–86.
[6] Kobayashi H, Hagiwara H, Kaneko H, Ogami Y. Effects of CO_2 dilution on turbulent premixed flames at high pressure and high temperature. Proc Combust Inst 2007;31:1451–8.
[7] Kobayashi H, Yata S, Ichikawa Y, Ogami Y. Dilution effects of superheated water vapor on turbulent premixed flames at high pressure and high temperature. Proc Combust Inst 2009;32:2607–14.
[8] Wang J, Matsuno F, Okuyama M, Ogami Y, Kobayashi H, Huang Z. Flame front characteristics of turbulent premixed flames diluted with CO_2 and H_2O at high pressure and high temperature. Proc Combust Inst 2013;34:1429–36.
[9] Brdar RD, Jones RM. GE IGCC technology and experience with advanced gas turbines. ger-4207. Schenectady, NY: GE Power Systems; 2000. p. 10.
[10] Hannemann F, Koestlin B, Zimmermann G, Haupt G. Hydrogen and syngas combustion: pre-condition for IGCC and ZEIGCC. Siemens AG Power Generation; 2005. p. 233. W8IN G.
[11] Natarajan J, Lieuwen T, Seitzman J. Laminar flame speeds of H_2/CO mixtures: effect of CO_2 dilution, preheat temperature, and pressure. Combust Flame 2007;151:104–19.
[12] Prathap C, Ray A, Ravi MR. Effects of dilution with carbon dioxide on the laminar burning velocity and flame stability of H_2–CO mixtures at atmospheric condition. Combust Flame 2012;159:482–92.
[13] Ratna Kishore V, Ravi MR, Ray A. Adiabatic burning velocity and cellular flame characteristics of H_2–CO–CO_2–air mixtures. Combust Flame 2011;158:2149–64.
[14] Krejci MC, Vissotski AJ, Ravi S, Metcalfe WJ, Keromnes A, Curran HJ, et al. Laminar flame speed measurements of

moist syngas fuel blends at elevated pressures and temperatures. In: Spring technical meeting of the central states section of the combustion institute 2012.
[15] Das AK, Kumar K, Sung C-J. Laminar flame speeds of moist syngas mixtures. Combust Flame 2011;158:345–53.
[16] Hu E, Huang Z, He J, Jin C, Zheng J. Experimental and numerical study on laminar burning characteristics of premixed methane-hydrogen-air flames. Int J Hydrog Energy 2009;34:4876–88.
[17] Tang C, Huang Z, Jin C, He J, Wang J, Wang X, et al. Laminar burning velocities and combustion characteristics of propane-hydrogen-air premixed flames. Int J Hydrog Energy 2008;33:4906–14.
[18] Bradley D, Gaskell PH, Gu XJ. Burning velocities, markstein lengths, and flame quenching for spherical methane-air flames: a computational study. Combust Flame 1996;104:176–98.
[19] Law CK, Sung CJ. Structure, aerodynamics, and geometry of premixed flamelets. Prog Energy Combust Sci 2000;26:459–505.
[20] Gu XJ, Haq MZ, Lawes M, Woolley R. Laminar burning velocity and Markstein lengths of methane-air mixtures. Combust Flame 2000;121:41–58.
[21] Kee RJ, Grcar JF, Smooke MD, Miller JA. A FORTRAN program for modeling steady, laminar, one-dimensional premixed flames. SNAD85–8240. Sandia National Laboratories; 1993.
[22] Kee RJ, Rupley FM, Miller JA. CHEMKIN II: a FORTRAN chemical kinetics package for the analysis of gas-phase chemical and plasma kinetics. SAND89-8009. Sandia National Laboratories; 1991.
[23] Davis SG, Joshi AV, Wang H, Egolfopoulos F. An optimized kinetic model of H_2/CO combustion. Proc Combust Inst 2005;30:1283–92.
[24] Li J, Zhao Z, Kazakov A, Chaos M, Dryer FL, Scire JJ. A comprehensive kinetic mechanism for CO, CH_2O, and CH_3OH combustion. Int J Chem Kinet 2007;39:109–36.
[25] Liang W, Chen Z, Yang F, Zhang H. Effects of soret diffusion on the laminar flame speed and Markstein length of syngas/air mixtures. Proc Combust Inst 2013;34:695–702.
[26] Chen Z. Effects of radiation and compression on propagating spherical flames of methane/air mixtures near the lean flammability limit. Combust Flame 2010;157:2267–76.
[27] Chen Z, Tang C, Fu J, Jiang X, Li Q, Wei L, et al. Experimental and numerical investigation on diluted DME flames: thermal and chemical kinetic effects on laminar flame speeds. Fuel 2012;102:567–73.
[28] Xie Y, Wang J, Zhang M, Gong J, Jin W, Huang Z. Experimental and numerical study on laminar flame characteristics of methane oxy-fuel mixtures highly diluted with CO_2. Energ Fuels 2013;27:6231–7.
[29] Qiao L, Kim C, Faeth G. Suppression effects of diluents on laminar premixed hydrogen/oxygen/nitrogen flames. Combust Flame 2005;143:79–96.
[30] Gu X, Li Q, Huang Z. Laminar burning characteristics of diluted n-Butanol/air mixtures. Combust Sci Technol 2011;183:1360–75.
[31] Landau L. On the theory of slow combustion. Acta Physicochimica URSS 1944;19:77–85.
[32] Vu TM, Park J, Kwon OB, Bae DS, Yun JH, Keel SI. Effects of diluents on cellular instabilities in outwardly propagating spherical syngas-air premixed flames. Int J Hydrog Energy 2010;35:3868–80.
[33] Sivashinsky GI. Instabilities, pattern formation, and turbulence in flames. Annu Rev Fluid Mech 1983;15:179–99.
[34] Bouvet N, Halter F, Chauveau C, Yoon Y. On the effective Lewis number formulations for lean hydrogen/hydrocarbon/air mixtures. Int J Hydrog Energy 2013;38:5949–60.
[35] Muppala SPR, Nakahara M, Aluri NK, Kido H, Wen JX, Papalexandris MV. Experimental and analytical investigation of the turbulent burning velocity of two-component fuel mixtures of hydrogen, methane and propane. Int J Hydrog Energy 2009;34:9258–65.
[36] Kwon OC, Rozenchan G, Law CK. Cellular instabilities and self-acceleration of outwardly propagating spherical flames. Proc Combust Inst 2002;29:1775–83.
[37] Yu JF, Yu R, Fan XQ, Christensen M, Konnov AA, Bai XS. Onset of cellular flame instability in adiabatic $CH_4/O_2/CO_2$ and CH_4/air laminar premixed flames stabilized on a flat-flame burner. Combust Flame 2013;160:1276–86.
[38] Yuan J, Ju Y, Law CK. On flame-front instability at elevated pressures. Proc Combust Inst 2007;31:1267–74.